Journal of Alloys and Compounds 509 (2011) 316–320

Contents lists available at ScienceDirect

Journal of Alloys and Compounds

journal homepage: www.elsevier.com/locate/jallcom

Growth and optical properties of tetrapod-like indium-doped ZnO nanorods with a layer-structured surface

Fangping Cai, Liping Zhu*, Haiping He, Jiesheng Li, Yefeng Yang, Xiaojun Chen, Zhizhen Ye

State Key Laboratory of Silicon Material, Department of Materials Science and Engineering, Zhejiang University, Zheda Road 38, Hangzhou 310027, PR China

ARTICLE INFO

Article history:
Received 21 June 2010
Received in revised form 1 September 2010
Accepted 1 September 2010
Available online 15 September 2010

Keywords:
Nanostructure
Crystal structure
Chemical vapor deposition
Photoluminescence

ABSTRACT

We report tetrapod-like indium-doped ZnO nanorods with a layer-structured surface, synthesized by a thermal vapor transport method. The high crystalline quality of the nanostructure sample obtained was confirmed by using X-ray diffraction, scanning electron microscopy and transmission electron microscopy. We carried out photoluminescence and photoluminescence excitation measurements to investigate the possible application of this indium-doped ZnO nanostructure in the field of optical devices. The photoluminescence exhibited an ultra strong visible wavelength emission with a peak intensity 300 times stronger than the band edge ultraviolet emission. In addition, a very slow decay of visible wavelength emission was revealed by time-resolved photoluminescence spectroscopy.

1. Introduction

ZnO nanostructures have attracted much attention as they are oxide semiconductor materials with a wide and direct band-gap of 3.3 eV and a high exciton binding energy of 60 meV [1–3], which properties are required to develop bright emitters and phosphors in the ultraviolet. A variety of nanostructured ZnO materials including nanowires, nanobelts, core–shell nanostructures, chestnut-like nanostructures and nano-composites have been synthesized [4–14]. As we know, doping ZnO with selected elements offers an effective way to adjust their electrical, optical, and magnetic properties, which is important for practical applications [15–23]. By doping ZnO films with indium (In), the Fermi level, work function, and conductivity can be modified [24,25] for the realization of light-emitting and field-emitting devices. It has also been found that the introduction of In can give rise to dramatic changes in the morphologies of nanostructures [26–28].

It has been established that visible emission is much weaker than band edge emission for bulk ZnO and thin ZnO films of high crystal quality [29–33]. In ZnO nanostructures, however, the intensity of the defect emission can be several orders of magnitude stronger than that of the band edge emission, due to the nanostructures' increased surface-to-volume ratio. This is because surface defects make a significant contribution to visible emission [34–38]. It has been reported that sulfur doping enhances the visible emission from ZnO nanowires, giving a large peak intensity ratio of 400 at room temperature, indicating the potential optoelectronic applications of the visible emission [39–41].

In previous studies [42,43], we succeeded in obtaining Al-doped ZnO nanorods and observed their field emission and it was thought it would be interesting to extend this work to the In-doping system. While attempting to prepare In-doped ZnO nanowire or nanorods to improve their electrical properties so as to be suitable for use in field emission devices, we unexpectedly obtained novel tetrapod-like indium-doped ZnO nanorods with a layer-structured surface, which showed ultra strong visible emission. In this letter, we report the growth and characterization of this In-doped ZnO nanostructure. Using time-resolved photoluminescence techniques, a very slow decay of visible wavelength emission was observed, and the role of In doping in producing the visible emission was assessed.

2. Experimental details

The synthesis of tetrapod-like indium-doped ZnO nanorods with a layer-structured surface was conducted using a simple directly thermal evaporation method in a horizontal quartz tube furnace without a catalyst [44]. Pure metal zinc powder (99.999%) and an indium droplet (99.999%) mixture with a molar ratio of 90:10 were used as the source materials and they were put in a quartz boat covered with a similar one to maintain the vapor pressure. A clean Si (0 0 1) wafer was placed downstream as the substrate. The growth process was divided into two steps. First, the furnace was heated to a set temperature of 600 °C and the boat was then inserted in the furnace under a constant nitrogen flow of 50 sccm and kept there for 10 min. Second, the set temperature was raised to 800 °C and the carrier gas was changed to oxygen with a constant flow of 60 sccm and kept at that level for 30 min. Finally the boat was pulled out and cooled in the atmosphere.

X-ray diffraction (XRD) patterns were measured using a Bede D1 diffractometer using graphite monochromated Cu Kα (λ = 1.5418 Å) radiation. The morphology of the nanostructures was examined using a HITACHI S-4700 field emission scanning electronic microscope (FESEM) equipped with a GENESIS4000 energy dispersive

* Corresponding author. Tel.: +86 571 87953139; fax: +86 571 87952625.
E-mail addresses: zlp1@zju.edu.cn, zlp1@zjuem.zju.cdu.cn (L. Zhu).

0925-8388/$ – see front matter © 2010 Elsevier B.V. All rights reserved.
doi:10.1016/j.jallcom.2010.09.016

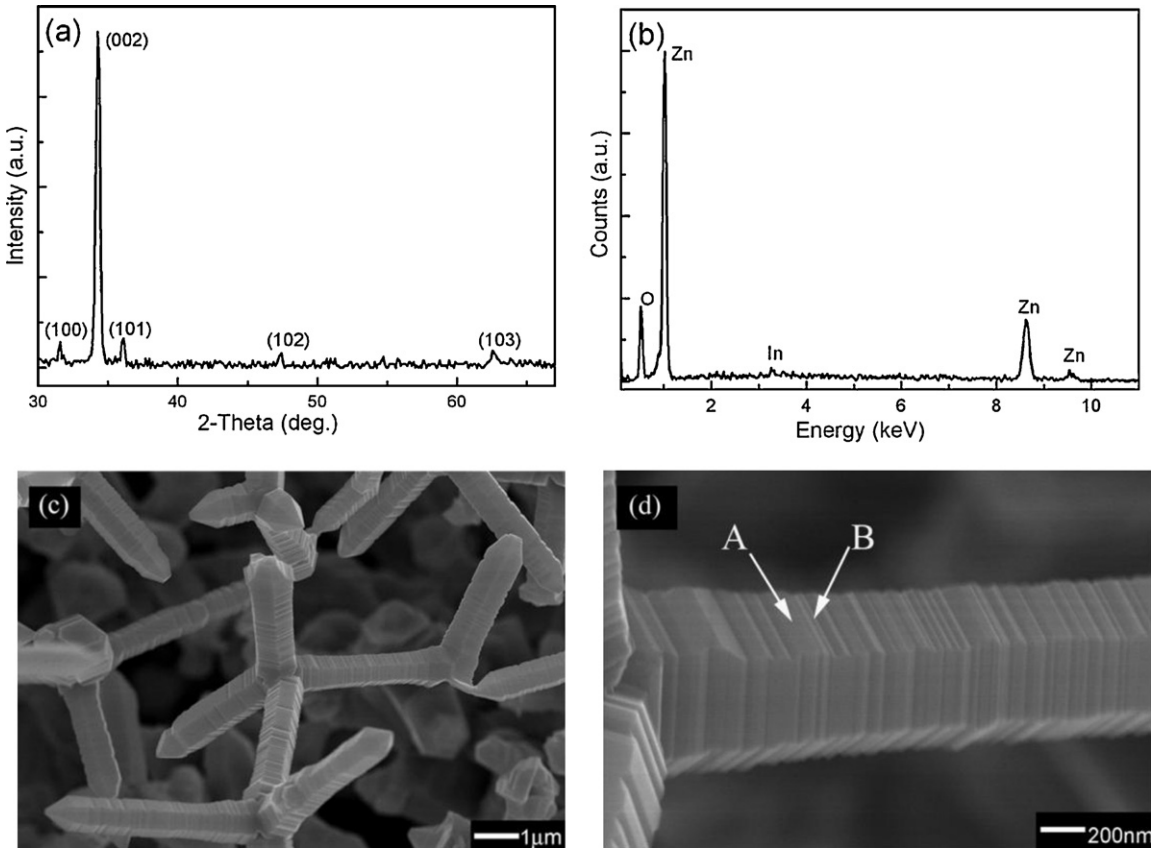

Fig. 1. (a) XRD pattern, (b) EDX measurement, (c) SEM image at low magnification and (d) SEM image at high magnification for the indium-doped ZnO nanostructures.

X-ray spectroscope (EDS) and JEM-2010 high resolution transmission electronic micro-spectroscope (HRTEM). Photoluminescence (PL) and photoluminescence excitation (PLE) measurements were performed on a FluoRoLOG-3-TAU (Jobin Yvon) fluorescence spectrometer at temperatures from 8 to 290 K; the excitation wavelength was 500 nm, produced by a xenon (Xe) lamp. A pulsed Xe lamp was used for PL decay. The pulse width was 3 μs and the tail of the pulse could be neglected.

3. Results and discussion

Fig. 1 shows the results of XRD, SEM and EDS measurements for the In-doped ZnO nanostructures obtained. All the refraction peaks in Fig. 1(a) could be indexed to wurtzite ZnO, and the appearance of a strong (0 0 0 2) peak indicated that it was highly oriented with the (0 0 0 1) direction. Doping using indium did not introduce other phases like metallic In or In_2O_3 in the XRD patterns. EDS data for the composition of the samples indicated that indium was doped into the ZnO tetrapod and the content was ~1.6 atom percent as shown in Fig. 1(b). The morphology of the sample showed a tetrapod-like shape with a layer-structured surface, as shown in Fig. 1(c) and (d). Every arm of the tetrapod-like nanostructure was longer than 2 μm and uniform along their length, and the component layers of the tetrapod's arms showed a hexagonal cross-section with a thickness of ~20 nm. Note that the surfaces of the tetrapod were not uniform.

The morphology and microstructure of the samples were further analyzed by TEM, as shown in Fig. 2(a). Clear parallel fringes with inter-planar spacing of 0.26 nm corresponding to the (0 0 0 2) plane could be observed. This indicated that the tetrapod was single crystalline and grew along the (0 0 0 1) direction, which corresponded with the XRD patterns, as shown in Fig. 1(a). Note that the uniform surfaces of the tetrapod could be differentiated into A and B areas. The former shows an evident local plane, and the latter shows a layer-structured shape. We also found that the B areas were much darker compared to the A sites. Fig. 2(c) shows the selected area diffraction (SAD) pattern of the indium-doped ZnO tetrapod. The SAD pattern further confirmed the growth orientation of the indium-doped ZnO tetrapod and indicated that these tetrapods were single crystalline. The quantitative EDS analysis of the B site in Fig. 2(d) revealed an indium concentration of ~2.0 atom per cent, a little higher than average.

Based on the above analysis, the distribution of the indium atoms was obviously important in concluding whether indium played a significant role in the formation of the nanostructure. So we carried out element line-by-line scanning measurements, the results of which are shown in Fig. 2(b). As we can see, the Zn and O elements were uniformly distributed in the nanorod, but the In seemed to be gathered together. It is suggested that the introduction of In^{3+} ion produced a structural stress because of the larger radius of the In^{3+} ion (0.08 nm) compared to that of Zn^{2+} ion (0.074 nm), so the aggregation of indium atoms in the ZnO nanorods minimized the structural stress.

The formation of the tetrapod-like nanostructure can be understood by the mechanism whereby multiply-twinned particles (MTP) incorporate small angle grain boundaries or stacking faults, which has been reported by Iijima [45] and Yu and co-workers [46] to explain the formation of tetrapod Si and tetrapod ZnO, respectively. The layer structure growth mechanism can be illustrated by the aggregation of the indium atoms. As we can see in Fig. 2(a), there is no obvious dislocation or stacking-faults but there is lattice deformation at the edge of the nanorods. The results of EDS and the element line-by-line scanning measurements indicate the aggregation of the indium atoms, which also happened in the In-doped ZnO nanobelts and ZnO ceramics [28,47]. Here we propose a detailed growth mechanism, as per the schematic diagram in Fig. 3. First,

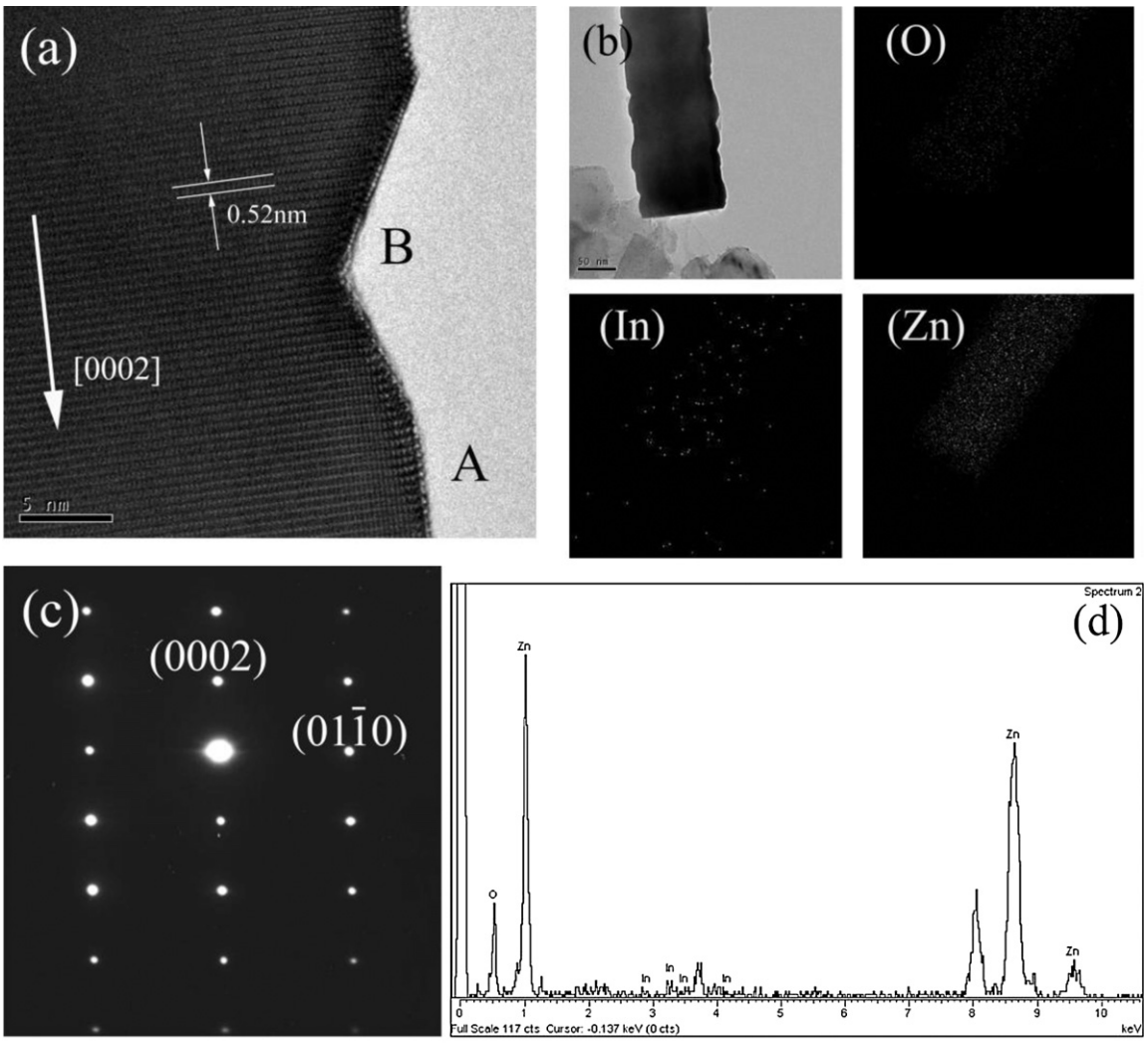

Fig. 2. (a) HRTEM image of the tetrapod arm of the indium-doped ZnO nanostructure, (b) element distribution by line-by-line scanning, (c) SAD pattern of the In-doped tetrapod's arm, and (d) EDS measurement for the "dark area" corresponding to the site B in (a).

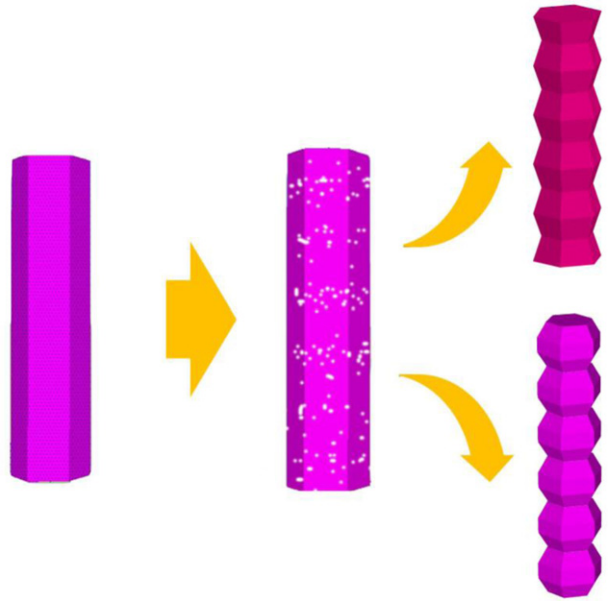

Fig. 3. Schematic illustration of the ZnO tetrapod-like layer structure growth mechanism.

the distribution of indium atoms was comparatively uniform as the growth began. Next, the doping with indium atoms induced lattice distortion because of the difference in the size of the radius, and the indium atoms tended to gather together to minimize the structural stress. Finally, the indium-rich area made the $(0\,\bar{1}\,1\,0)$ of the ZnO wurtzite structure disappear and collapse happened in the surface of the nanorods. The irregular array of the layer structures, as per the two results shown in Fig. 3, brought about non-uniform collapse, which coincided with the layer structure shown in Fig. 1(d).

Fig. 4(a) shows the PL spectra at room temperature for the In-doped ZnO nanostructures together with the undoped ZnO nanorods for comparison. Fig. 4(b) shows the PL spectra at different temperatures for the In-doped ZnO nanostructures. It can be seen that the two kinds of spectra in Fig. 4(a) are very different: the UV band-edge emission almost disappears, while the visible emission is very strong for the In-doped ZnO nanostructures. Note that the peak intensity ratio of the defect emission to the band edge emission is as large as 550 at room temperature, which is larger than the previously reported largest value of 400 for sulfur-doped ZnO nanowires [36]. The unprecedented ratio of defect to band edge emission reported here can be explained by the following three aspects. First, of course the nanostructure with a large surface-to-volume ratio in ZnO played an important role in the increase in the ratio of defect to band edge emission

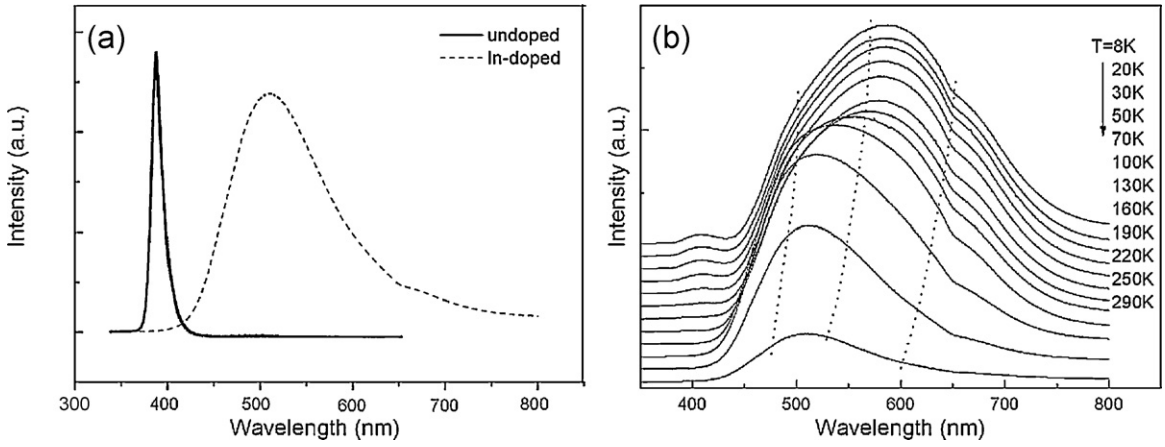

Fig. 4. (a) Photoluminescence spectrum at room temperature and (b) photoluminescence spectra in the temperature range of 8–290 K for the indium-doped ZnO nanostructure.

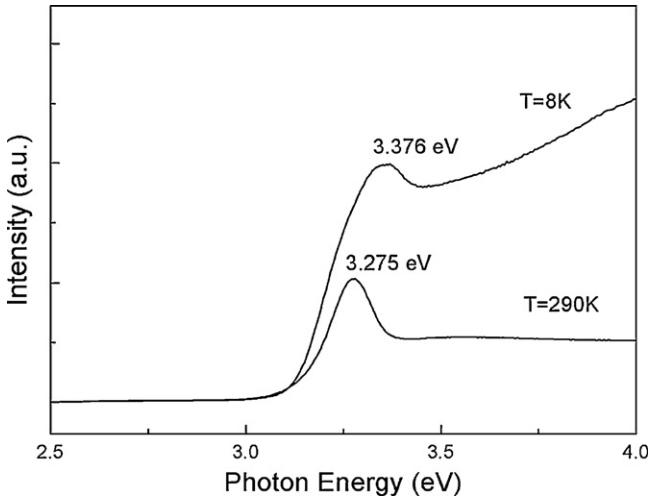

Fig. 5. Photoluminescence excitation spectroscopy at 8 K and 290 K for the indium-doped ZnO nanostructure.

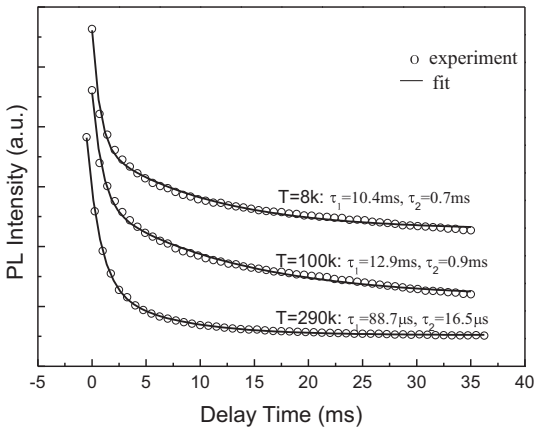

Fig. 6. Time-resolved photoluminescence decay of the defect emission at 8 K, 100 K and 290 K for the indium-doped ZnO nanostructure.

[37]. Second, the energy of the free exciton transfer to the defect state resulted in the weak intensity of band edge emission and the strong intensity of defect emission. This hypothesis can be confirmed by the results of the PLE spectroscopy, as shown in Fig. 5. An excitonic resonance was clearly observed at 3.275 eV and 3.376 eV in the absorption profiles measured at room temperature and 8 K respectively, which was attributed to free exciton states [48], indicating that the large intensity of defect emission benefited from the decrease in band edge emission. Third, the nonradiative recombination caused by indium doping dominated the band edge relaxation and enhanced the energy transfer from the band edge to the defect states responsible for visible emission, resulting in a reduced band edge emission and a much brighter visible emission. We also measured the time-resolved photoluminescence decay of the defect emission at 8 K, 100 K and 290 K, as shown in Fig. 6. It can be clearly observed that the experiment results are in good accordance with the fitted ones from the biexponential decay lifetimes formula of $I \sim A\exp(-t/\tau_1) + B\exp(-t/\tau_2)$, where I is the luminescence intensity, τ_1, τ_2 the lifetime, and A, B the constant. The average lifetime τ could be calculated [49] as 9.3 ms, 11.7 ms and 63.3 μs at 8 K, 100 K and 290 K, respectively. This green band (GB) lifetime had a maximum value of 11.7 ms at 100 K, but decreased quickly to 66.3 μs at 290 K, which was much longer than that of the band edge emission around 3.3 eV in ZnO (in orders of ~ps or ns) [50,51]. Such a long decay time of defect emission in order of ~ms has been reported [49,52,53], however, the mechanism is still not very clear.

4. Conclusions

In summary, tetrapod-like indium-doped ZnO nanorods with a layer-structured surface were synthesized by a thermal vapor transport method. The average content of indium reached 1.6 at.% and the indium in the nanostructures had an important effect on their structure and photoluminescent behavior. The irregular surfaces of the tetrapod's arms were caused by the asymmetrical distribution of indium atoms. The tetrapod-like indium-doped ZnO nanorods with a layer-structured surface showed ultra strong visible emission and ultra long life time, which may offer an opportunity for their application in engineering bright emitters and phosphors in the visible spectrum.

Acknowledgements

This work is supported by the "973" Program of China under Grant No. 2006CB604906, National Natural Science Foundation of China No. 50772099 and Doctoral Fund of Ministry of Education of China under Grant No. 20090101110044.

References

[1] S.N. Das, K.J. Moon, J.P. Kar, J.H. Choi, J. Xiong, T.I. Lee, J.M. Myoung, Appl. Phys. Lett. 97 (2010) 022013.

[2] H.G. Chen, S.R. Jian, Z.W. Li, K.W. Chen, J. Alloys Compd. 4 (2010) 21843.
[3] G. Meng, X.D. Fang, Y.K. Zhou, J.U. Seo, W.W. Dong, S. Hasegawa, H. Asahi, H. Tambo, M.G. Kong, L. Li, J. Alloys Compd. 491 (2010) 72–76.
[4] Z.W. Pan, Z.R. Dai, Z.L. Wang, Science 83 (2001) 2061.
[5] X. Lin, X.B. He, T.Z. Yang, W. Guo, D.X. Shi, H.J. Gao, D.D.D. Ma, S.T. Lee, F. Liu, X.C. Xie, Appl. Phys. Lett. 89 (2006) 043103.
[6] X. Wu, F.Y. Qu, X. Zhang, W. Cai, G.Z. Shen, J. Alloys Compd. 486 (2009) L13–L16.
[7] Y.J. Fang, Y.W. Wang, Y.T. Wan, Z.L. Wang, J.A. Sha, J. Phys. Chem. C 114 (2010) 12469–12476.
[8] H.Y. Yang, S.F. Yu, J. Yan, L.D. Zhang, Appl. Phys. Lett. 96 (2010) 141115.
[9] A. Asthana, K. Momeni, A. Prasad, Y.K. Yap, R.S. Yassar, Appl. Phys. Lett. 95 (2009) 172106.
[10] Y. Myung, D.M. Jang, T.K. Sung, Y.J. Sohn, G.B. Jung, Y.J. Cho, H.S. Kim, J. Park, Acs. Nano 4 (2010) 3789–3800.
[11] L.L. Yang, Q.X. Zhao, M. Willander, J. Alloys Compd. 469 (2009) 623–629.
[12] S.L. Wang, X. Jia, P. Juang, H. Fang, W.H. Tang, J. Alloys Compd. 502 (2010) 118–122.
[13] Y.L. Tao, M. Fu, A.L. Zhao, D.W. He, Y.S. Wang, J. Alloys Compd. 489 (2010) 99–102.
[14] B. Kulyk, V. Kapustianyk, V. Tsybulskyy, O. Krupka, B. Sahraoui, J. Alloys Compd. 502 (2010) 24–27.
[15] D.Y. Wang, J. Zhou, G.Z. Liu, J. Alloys Compd. 487 (2009) 545–549.
[16] L. Luo, L. Gong, Y.F. Liu, J. Chen, C.R. Ding, X.G. Tang, X.L. Li, Z.R. Qiu, H.Z. Wang, X.M. Chen, K.F. Li, H.H. Fan, K.W. Cheah, Opt. Mater. 32 (2010) 1066–1070.
[17] J.H. Yang, X.Y. Liu, L.L. Yang, Y.X. Wang, Y.J. Zhang, J.H. Lang, M. Gao, M.B. Wei, J. Alloys Compd. 485 (2009) 743.
[18] X.Y. Xu, C.B. Cao, J. Alloys Compd. 501 (2010) 265–268.
[19] L.P. Zhu, M.J. Zhi, Z.Z. Ye, B.H. Zhao, Appl. Phys. Lett. 88 (2006) 113106.
[20] T.H. Fang, S.H. Kang, J. Alloys Compd. 492 (2010) 536–542.
[21] S.H. Huang, Q. Xiao, H. Zhou, D. Wang, W.J. Jiang, J. Alloys Compd. 486 (2009) L24–L26.
[22] M.D. McCluskey, S.J. Jokela, J. Appl. Phys. 106 (2009) 071101.
[23] J.S. Jie, G.Z. Wang, X.H. Han, Q.X. Yu, Y. Liao, G.P. Li, J.G. Hou, Chem. Phys. Lett. 387 (2004) 466.
[24] D.C. Reynolds, D.C. Look, B. Jogai, C.W. Litton, G. Cantwell, W.C. Harsch, Phys. Rev. B 60 (1999) 2340.
[25] M.X. Jung, E.S. Lee, E.I. Jeon, K.S. Gil, J.J. Kim, Y. Murakami, S.H. Lee, H.J. Lee, T. Yao, H. Makino, J.H. Chang, J. Alloys Compd. 481 (2009) 649.
[26] H.J. Fan, A.S. Barnard, M. Zacharias, Appl. Phys. Lett. 90 (2007) 143116.
[27] J.Y. Lao, J.Y. Huang, D.Z. Wang, Z.F. Ren, Nano Lett. 3 (2003) 235.
[28] Y. Ding, X.Y. Kong, Z.L. Wang, Phys. Rev. B 70 (2004) 235408.
[29] J.G. Lu, Z.Z. Ye, F. Zhuge, Y.J. Zeng, B.H. Zhao, L.P. Zhu, Appl. Phys. Lett. 85 (2004) 3134.
[30] J.H. Yang, J.H. Lang, L.L. Yang, Y.J. Zhang, D.D. Wang, H.G. Fan, H.L. Liu, Y.X. Wang, M. Gao, J. Alloys Compd. 450 (2008) 521–524.
[31] G.D. Yuan, Z.Z. Ye, L.P. Zhu, Q. Qian, B.H. Zhao, S.B. Zhang, Appl. Phys. Lett. 86 (2005) 202106.
[32] F. Zhuge, L.P. Zhu, Z.Z. Ye, J.G. Lu, J.Y. Huang, F.Z. Wang, Appl. Phys. Lett. 87 (2005) 092103.
[33] L.L. Chen, J.G. Lu, Z.Z. Ye, Y.M. Lin, B.H. Zhao, Y.M. Ye, J. Li, L.P. Zhu, Appl. Phys. Lett. 87 (2005) 252106.
[34] L.E. Greene, M. Law, J. Goldberger, F. Kim, J.C. Johnson, Y. Zhang, R.J. Saykally, P. Yang, Angew. Chem. Int. Ed. 42 (2003) 3031.
[35] N.E. Hsu, W.K. Huang, Y.F. Chen, J. Appl. Phys. 96 (2004) 4671.
[36] X. Liu, X. Wu, H. Cao, R.P.H. Chang, J. Appl. Phys. 95 (2004) 3141.
[37] I. Shalish, H. Temkin, V. Naracanamurti, Phys. Rev. B 69 (2004) 245401.
[38] G. Meng, X.D. Fang, Y. Zhou, J. Seo, W.W. Dong, S. Hasegawa, H. Asahi, H. Tambo, M. Kong, L. Li, J. Alloys Compd. 491 (2010) 72–76.
[39] S.Y. Bae, H.W. Seo, J. Park, J. Phys. Chem. B 108 (2004) 5206.
[40] B.Y. Geng, G.Z. Wang, Z. Jiang, T. Xie, S.H. Sun, G.W. Meng, L.D. Zhang, Appl. Phys. Lett. 82 (2003) 4791.
[41] J.V. Foreman, J. Li, H. Peng, S. Choi, H.O. Everitt, J. Liu, Nano Lett. 6 (2006) 1126.
[42] H.P. He, H.P. Tang, Z.Z. Ye, L.P. Zhu, B.H. Zhao, L. Wang, X.H. Li, Appl. Phys. Lett. 90 (2007) 023104.
[43] H.P. Tang, L.P. Zhu, H.P. He, Z.Z. Ye, Y.Z. Zhang, M.J. Zhi, Z.X. Yang, B.H. Zhao, T.X. Li, J. Phys. D 39 (2006) 2696.
[44] M.J. Zhi, L.P. Zhu, Z.Z. Ye, F.Z. Wang, B.H. Zhao, J. Phys. Chem. B 109 (2005) 23930.
[45] S. Iijima, Jpn. J. Appl. Phys. Part 1 26 (1987) 357–364.
[46] Y. Zhang, H.B. Jia, X.H. Luo, X.H. Chen, D.P. Yu, R.M. Wang, J. Phys. Chem. B 107 (2003) 8289–8293.
[47] C. Li, Y. Bando, M. Nakamura, N. Kimizuka, Micron 31 (2000) 543.
[48] L. Wang, N.C. Giles, J. Appl. Phys. 94 (2003) 973.
[49] H.P. He, Z.Z. Ye, S.S. Lin, B.H. Zhao, J.Y. Huang, J. Phys. Chem. C 112 (2008) 14262–14265.
[50] C.R. Hall, L.V. Dao, K. Koike, S. Sasa, H.H. Tan, M. Inoue, M. Yano, C. Jagadish, J.A. Davis, Appl. Phys. Lett. 96 (2010) 193117.
[51] Q.X. Zhao, L.L. Yang, M. Willander, B.E. Sernelius, P.O. Holtz, J. Appl. Phys. 104 (2008) 073526.
[52] G.Q. Tang, Y. Xiong, L.Z. Zhang, G.L. Zhang, Chem. Phys. Lett. 395 (2004) 97.
[53] T.H. Fang, Y.S. Chang, L.W. Ji, S.D. Prior, W. Water, K.J. Chen, F.F. Fang, C.N. Fang, S.T. Shen, J. Phys. Chem. Solids 70 (2009) 1015.